Time-resolved imaging of spatiotemporal patterns in a one-dimensional dielectric-barrier discharge system

M. Klein, N. Miller, and M. Walhout[*]

Department of Physics and Astronomy, Calvin College, Grand Rapids, Michigan 49546

A makeshift streak camera produces time-resolved images of filament patterns in a one-dimensional dielectric-barrier discharge system. The images reveal a variety of spatial and temporal structures, including temporally distinct discharge stages that occur at specific phases of the 12.5 kHz driving oscillation and spatially periodic filament arrays that are generated during the discharge stages. The data answer recent questions regarding time-averaged images of a similar system. Most notably, all but the simplest time-averaged images are due to the integration of multiple filament patterns generated in different discharge stages. Disordered states of the system are also examined. Some of these are spatially disordered but display temporal structure; others appear to lack both spatial and temporal order. Possibilities are suggested for investigations of surface-charge spreading and pattern stability in similar systems.

High-pressure, ac-driven, dielectric-barrier discharge (DBD) systems are capable of generating nonequilibrium energy distributions in gases while being operated quasicontinuously. As a result, they have proven useful in laboratory and industrial applications requiring the production of ultraviolet radiation and reactive chemical species [1–3]. Their utility in these applications can be traced to the behavior of individual microdischarges, or filaments, an array of which is generated with each half cycle of the driving oscillation. To date, little attention has been paid to controlling and/or exploiting the spatial or temporal *distributions* of DBD filaments in plasma applications. This is probably due to the complexity and variability of filament arrays in the most common DBD configurations. This paper examines an effectively one-dimensional (1D) DBD system that supports a variety of spatial and temporal structures that are simple enough to be understood and stable enough to be of possible interest in DBD applications.

The evolution of any single DBD filament is determined by the applied electric field and by the modification of the local field due to charges originating in the filament itself. In the configuration to be considered here, free charge is never able to escape the system via either electrode. Rather, it accumulates on dielectric surfaces that cover both electrodes and serve as barriers to conduction. The charge accumulating at the ends of a filament produces a field that opposes the applied field—an effect that results in the local field falling below the discharge-sustaining level and the filament becoming extinguished only about 20 ns after its initiation. However, since the charge and the attenuated field are localized, additional filaments may form just a short distance from the original filament site, where the field remains above breakdown. In typical DBD systems, multiple filaments can fire in a relatively small area, but seldom do extended filament patterns stabilize in any repeatable way.

In the 1D system to be examined here, arrays of filaments form stable, spatially periodic patterns, with filaments firing repeatedly at the same, regularly spaced locations for more than 10^5 DBD cycles. The goal of this paper is to report on short-term behavior that contributes to this long-term structure. As will be described, we have obtained images of our system with time resolution on scales much shorter than the driving period. The images reveal that patterned arrays appear in ''bursts,'' or ''discharge stages,'' each lasting only ~100 ns. More importantly, we find that several discharge stages may occur during a single half cycle of the driving oscillation, each producing a distinct filament pattern. Our images provide a means of analyzing and interpreting time-averaged filament patterns that have been reported recently [4] and are typically seen by the unaided eye. They also help delineate the qualitative boundary between ordered and disordered behavior in our 1D DBD. This work has enhanced our understanding of pattern-formation dynamics in this system and points to the emerging possibility that filament patterns could serve as a useful DBD diagnostic.

As indicated in Fig. 1, the discharge takes place in a narrow, cylindrical glass tube, with an inner diameter of 2.0 mm, an outer diameter of 7.8 mm, and a length of 38 cm. Two stripes of silver, 3 mm wide, are painted on diametrically opposite sides of the tube's outer surface. These electrodes extend out of opposite ends of an insulating jacket that prevents unwanted discharging around the outside of the tube. A function generator supplies a 12.5 kHz sinusoidal voltage signal, which is sent through an audio amplifier (with adjustable gain), stepped up by a high-voltage transformer, and applied to the electrodes. Circuit elements are selected so that the voltage across the tube [$V = V_0 \sin(\omega t)$] is in phase with the voltage across a series capacitor (V_C), which is assumed proportional to the charge stored on the electrodes. A simple gas manifold is used to control the mixing ratio, flow rate, pressure, and purity of a helium-argon mixture in the discharge tube. A variety of filament patterns are observed for different gas parameters and voltage amplitudes [4].

A makeshift streak camera provides microsecond time resolution along the vertical axes of our images and better than 0.1 mm spatial resolution along the horizontal. The im-

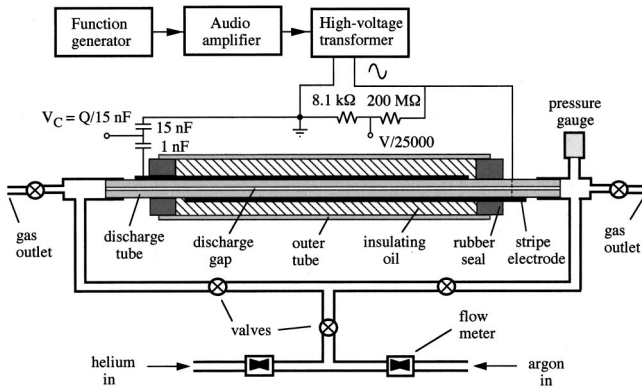*Author to whom correspondence should be addressed.

FIG. 1. Diagram of the DBD setup. The helium-to-argon ratio of flowing gas is monitored with flow meters. Valves are used in various combinations to purge or seal the system or to balance the flow of gas in the discharge gap. The pressure gauge (MKS baratron) provides a species-independent measure of the gas pressure. Electrical components in the DBD circuit are chosen so that the applied voltage (V) is in phase with the charge (Q) stored on the electrodes. An estimated possible error of 5% should be assumed for the voltage amplitude V_0, owing to the high-voltage extrapolation of the voltage-divider calibration.

aging system, shown schematically in Fig. 2, relies on a ten-sided optical polygon that rotates at a frequency of 125 Hz and sweeps an image of the discharge tube across the face of a charge-coupled device (CCD) video camera every 800 μs (ten discharge cycles). The polygon rotation is phase locked to the DBD drive through a divide-by-100 counter stage, so that the camera captures every tenth cycle of the discharge. The imaging system intercepts about 2° of the 36° sweep angle and therefore registers information over a time window of just 50 μs. An electronic delay built into the phase lock allows this window to be moved to any portion of the DBD cycle. The lock is stable enough that, on time scales of many
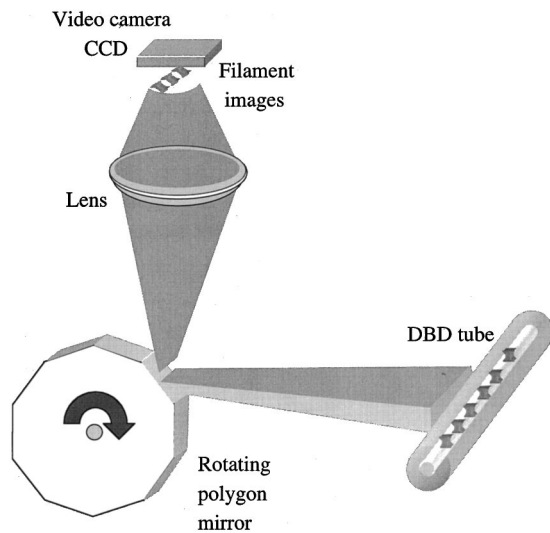

FIG. 2. Diagram of optical system for time-resolved imaging. The rotating optical polygon is phase locked to the DBD driving signal, so that every vertical position on the camera image is correlated with a particular phase of the DBD oscillation.
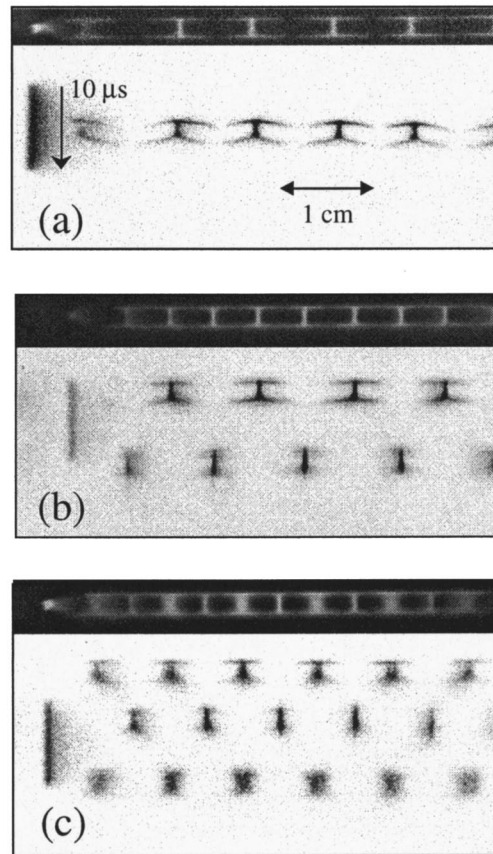

FIG. 3. Time-resolved images of three common patterns. At the top of each image a white-on-black, time-averaged picture of the discharge is shown, corresponding to what is seen by the unaided eye. The negative (black-on-white) images contain temporal information, with time increasing in the downward direction. The time scale is indicated by a light-emitting diode that is turned on for 10 μs and leaves a vertical streak on the left side of each image, starting when the voltage on the bottom electrode goes from negative to positive. Temporal and spatial scales are similar for all three images. (Note that filaments near the edges of the frames appear distorted because of the limitations of our imaging system, not because of instability or irregularity in the discharge patterns.) Images (a), (b), and (c) (with $V_0 = 460$, 800, and 1000 V) respectively correspond to pattern types A, B, and C identified in [4]. They were obtained with gas pressures in the range 760 ± 20 Torr (maintained at ~ 20 Torr above atmosphere). The Ar:He number-density ratio is 1:3 for image (a), 4:3 for (b), and 5:3 for (c). In image (c), the onset of the first discharge stage occurs in opposition to the applied voltage. This fact indicates that the local electric field is strongly affected by the surface-charge "footprint" remaining from the preceding cycle.

seconds, every vertical position on the camera image is a direct mapping of a particular temporal phase of the DBD cycle. Thus, no phase locking or precise positioning of the CCD is necessary, and a relatively long (typically $\frac{1}{30}$ s) exposure time can be used.

Three examples of time-resolved patterns are shown in Fig. 3. At the top of each image we provide a time-averaged picture of the discharge taken without the polygon spinning. These pictures closely resemble what is seen with the un-

aided eye, with filaments appearing as bright, vertical stripes that widen at the discharge tube wall. Time-resolved images are shown with negative shading (dark filaments against a bright background) and with time increasing along the downward vertical direction. We note that the vertical axis also contains some spatial information related to the vertical extent of the discharge filaments. However, separating temporal from spatial information is not a difficult task if one takes into account the brief duration of individual filaments and the distinctly flared filament shape at the tube wall. The typical discharge stage occurs so quickly that the sweeping mirror is virtually stationary for its duration, and we obtain a spatially well-resolved image of the stage's filament pattern. Subsequent discharge stages may take place several microseconds later, after the mirror has swept the tube image to a lower portion of the CCD array.

The high degree of stability of our DBD and imaging system is manifest in the high definition of imaged filaments. The time-resolved images in Fig. 3 were obtained for exposures of 0.033 s and therefore represent time-resolved, spatial averages over more than 400 DBD cycles (with a $\frac{1}{10}$ sampling fraction). Such a scheme can produce high-resolution images only if filaments fire repeatedly at the same locations and at the same temporal phases of the DBD driving oscillation.

Images (a), (b), and (c) in Fig. 3 show patterns obtained in three different ranges of driving amplitude V_0. Using the convention of [4], we classify the time-averaged images as type A, B, and C patterns, respectively. In our earlier work we demonstrated that the system made an abrupt transition from a type A pattern to a type B pattern as V_0 was increased enough to introduce a second discharge stage in every voltage half cycle. Similarly, the type C pattern appeared at even higher voltages after the onset of a third discharge stage in each half cycle. The presence of one, two, and three discharge stages for the different pattern types was detected in the form of kinks in an oscilloscope trace of V_C, which replicates the time dependence of stored charge. Our method did not enable us to determine which parts of the time-averaged pattern were formed during the different stages. Now, however, our time-resolved images make the situation clear. In Fig. 3(b) we see that type B patterns result from the interleaving of two patterns, which have similar periodicity but are offset by half a spatial period and form sequentially in successive discharge stages. The type C pattern contains a similar interleaving, but it exhibits a third pattern overlapping that formed in the first discharge stage of the half cycle. Together, the overlapping patterns of the first and third stages produce a characteristically wide filament image when time averaged. Thus, these experiments give unambiguous answers to questions regarding the qualitative spatiotemporal structure of our 1D DBD patterns.

The observed discharge behavior can be understood in terms of the qualitative model outlined in [4]. The stability of all filament patterns is first of all due to the "memory" effect caused by the surface-charge modifications of the local electric field. A patch of charge deposited during one voltage half cycle causes a field enhancement during the subsequent half cycle (after the local field has changed sign). The location of
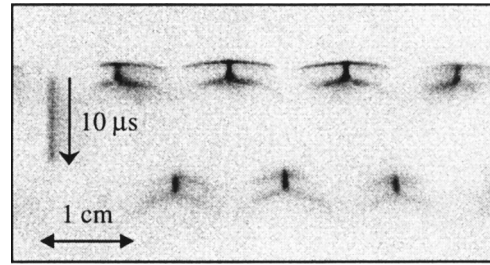

FIG. 4. Time-resolved spreading of filament feet. The flared ends (feet) of the discharge filaments in this type B pattern appear to droop downward, indicating a transverse spreading rate of roughly 0.5 mm/μs. The Ar:He ratio is 5:12, and the driving voltage amplitude is $V_0 = 700$ V. The "droop effect" is also observable in Fig. 3(a), but is not resolvable in the majority of our data.

this patch is therefore a probable site for a "return" discharge. This mechanism stabilizes the single-discharge-stage, type A patterns for driving amplitudes up to a transition voltage $V_{A \rightarrow B}$. At this amplitude, the field midway between adjacent filaments exceeds the breakdown value, and the second discharge stage commences. The present results demonstrate that the type B pattern is in fact an interleaving of first- and second-stage patterns and not a single, closely spaced filament pattern that is repeated with each discharge stage. While the latter possibility seemed remote in the context of our simple surface-charge model, it could not be eliminated until now.

A similar clarification emerges with respect to type C patterns. It was previously undetermined which, if any, of the wide and narrow filaments in the time-averaged, type C images were firing repeatedly during each half cycle. We now see that such repetition occurs only at the locations of wide filaments. This fact can be understood in terms analogous to the explanation of the $A \rightarrow B$ transition. Type C patterns occur when the voltage increases to the point of initiating a third discharge stage, with new filaments firing halfway between the filament sites of the second stage. This implies, of course, that the positions of the first- and third-stage filaments coincide. It is likely that the lingering effects of the first discharge stage influence the dynamics of the third discharge stage, possibly resulting in the unusual widths of (alternate) type C filaments. Understanding this influence in detail will require further experimental investigation and modeling.

Our imaging technique points the way toward obtaining information on the short-term spreading of the surface charges ("charge footprints") deposited by DBD filaments. Figure 4 [as well as Fig. 3(a)] shows filaments with flared ends, or "feet," that droop downward, indicating a relatively slow lateral spreading of the discharge after the filament is extinguished. We conjecture that the illumination at the tube wall maps out the positions at which charge is being deposited at different times. If this is the case, then we may interpret the drooping filament feet to be produced by the deposition of charge at the edges of the feet. We note that the top (cathode) feet and bottom (anode) feet of type A filaments are often very similar in size and spreading rate. In the case of type B patterns, this similarity seems to hold within the
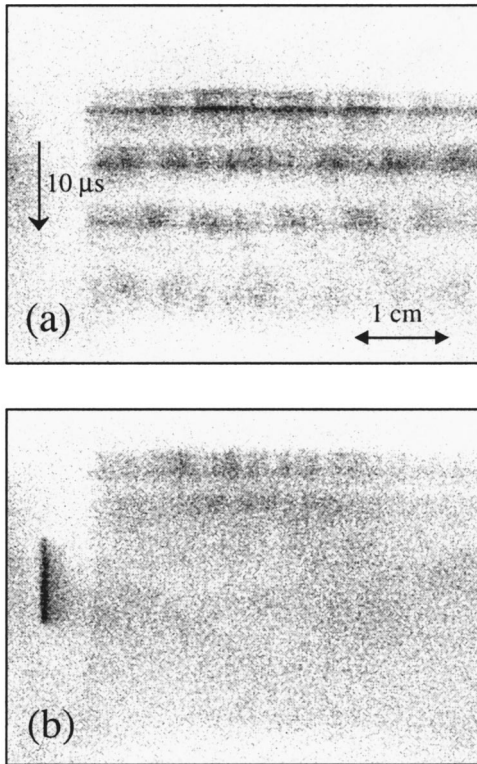
FIG. 5. These two spatially disordered states of the system, obtained with nearly identical gas and voltage settings, exhibit different degrees of temporal order. In image (a), at least three distinct discharge stages are visible. Image (b) shows significantly more disorder in the temporal behavior of filaments.

second discharge stage but breaks down for the first stage. In the first discharge stage in Fig. 4, for instance, the bottom feet have less lateral extent and perhaps more vertical extent than the top feet. These differences suggest that the character of the discharge at the tube wall and the charge-deposition process may be qualitatively different in the cases of A and B type patterns. Filament feet in type C patterns display still other variations that have not been fully investigated or understood. While our present system has demonstrated the feasibility of imaging the temporal spreading of discharge feet, the drooping effect is absent over most of the range of V_0. We plan to pursue a more extensive investigation of the effect in the future, employing better time resolution, a lower DBD driving frequency, and/or different gases.

The degree of disordered behavior in apparently chaotic states of our DBD was addressed briefly in [4]. Here we can add a few comments. For a small range of driving amplitudes between those producing type B and type C patterns, and for very large amplitudes, filaments fire at apparently random positions. Our previous work demonstrated that temporal disorder (the absence or degradation of distinct discharge stages) accompanies this spatial disorder in the system. Time-resolved images like those of Fig. 5 confirm this behavior but allow one to evaluate the degree of temporal disorder more carefully. In Fig. 5(a) we see a spatially disordered system that retains much of its temporal structure yet exhibits some temporal disorder, with scattered filaments ap-
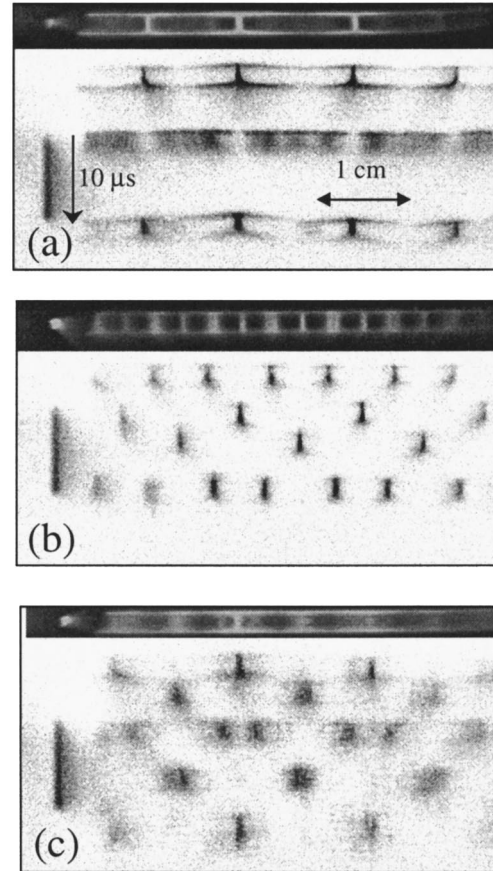

FIG. 6. More complex patterns. (a) This pattern was obtained with Ar:He ratio of 5:3 and $V_0 = 1250$ V. It appears to be a modified type C pattern, stabilizing out of the disorder that develops when V_0 is raised beyond the range for type B patterns. It is found over a ~ 100 V range of V_0 in very pure argon-dominated Ar-He mixtures. (b) This image was taken for $V_0 = 1020$ V and an Ar:He ratio of 4:3 (with trace impurities). The four-stage pattern often shows up over a very small range of V_0 as the system undergoes a transition from a type B to a type C pattern. Note that the time-resolved image reveals a spatial period twice as large as what is immediately seen by the unaided eye. (b) This five-stage pattern was seen in argon (with trace impurities) for $V_0 = 1320$ V. It appears to be the result of a narrow window of stability in a normally disordered range of V_0. The pattern is reproducible, but not easily so.

pearing outside still-identifiable discharge stages. The image in Fig. 5(b) reveals much less temporal structure than that in Fig. 5(a), even though the two were obtained under nearly identical conditions. We have observed that this kind of variability in the system occurs in an unpredictable way, but we suspect that it may be related to small changes in gas pressure and/or the introduction of a trace impurity in the gas.

While our gas manifold allows us to balance the amounts of He and Ar effectively and to purge the system easily and quickly, we are unable to control the small impurities that may escape from the discharge tube wall, internal valve parts, or any other part of the system. Fortunately, changes in the color of the discharge bespeak the presence of impurities, and a trace of air or nitrogen in the discharge produces a

bluish glow in the insulating oil jacket that surrounds the tube. It takes several minutes following a purge of the system before these indicators become obvious, so there is sufficient time for data acquisition with relatively pure discharging gas. Surprisingly, however, our experience shows that the stability of certain patterns—type C especially—is noticeably enhanced by the presence of trace impurities. As yet we have no detailed understanding of the mechanism by which such slight changes can influence the patterns so strongly.

As a last point, we note that time-resolved imaging has given us a way of identifying and distinguishing between complex patterns that are otherwise difficult to recognize. The images in Fig. 6 are examples of patterns that, when time averaged, appear as if they might be unstable versions of patterns we have already identified. But with time resolution we see that the patterns harbor unanticipated complexity in their spatiotemporal structures. The fact that such structures typically arise under very specific conditions, sometimes near a transition between stable states of the system, suggests that they may provide important clues to the under-lying pattern-formation dynamics. We will consider them carefully in our ongoing efforts to develop a quantitative model of 1D filament patterns.

The technique and results reported here mark a significant step in the process of analyzing and understanding spontaneous pattern formation in DBD's. We hope our work will prompt theoretical effort directed toward establishing a link between the microscopic conditions inside DBD filaments and the macroscopic patterns in which the filaments are organized. Such a link would be of considerable interest in the field of nonlinear dynamics, and it might prove beneficial in DBD applications. Moreover, we hope that the discharge stability demonstrated here raises interest in the immediate applicability of our DBD geometry in the controlled generation of chemical species or ultraviolet (possibly laser) radiation.

[1] B. Eliasson and U. Kogelschatz, IEEE Trans. Plasma Sci. **19**, 1063 (1991).

[2] U. Kogelschatz, B. Eliasson, and W. Egli, J. Phys. IV **7**, C4-47 (1997).

[3] U. Kogelschatz, B. Eliasson, and W. Egli, Pure Appl. Chem. **71**, 1819 (1999).

[4] J. Guikema, N. Miller, J. Niehof, M. Klein, and M. Walhout, Phys. Rev. Lett. **85**, 3817 (2000).